PHILOSOPHICAL TRANSACTIONS OF THE ROYAL SOCIETY A MATHEMATICAL, PHYSICAL & ENGINEERING SCIENCES

Unimolecular Reactions, Rates and Quantum State Distribution of Products

R. A. Marcus

Phil. Trans. R. Soc. Lond. A 1990 **332**, 283-296
doi: 10.1098/rsta.1990.0115

Unimolecular reactions, rates and quantum state distribution of products

By R. A. Marcus

Noyes Laboratory of Chemical Physics, California Institute of Technology, Pasadena, California 91125, U.S.A.

Microcanonical rates and products rovibrational quantum state distributions of several unimolecular dissociations, and canonical rates of some bimolecular associations, are discussed from the viewpoint of variational Rice–Ramsperger–Kassel–Marcus (RRKM) theory. The results are compared with the experimental data and with the very useful benchmark theory, phase space theory. A two-transition-state description is discussed for the threshold regions for the products vibrational excitations.

1. Introduction

In a unimolecular dissociation, and in the reverse process of free radical recombination, there is often no local maximum in the potential energy curve. In this case, and in others, a variational method for determining the position of the transition state has been used. In a recent series of studies variational RRKM theory has been applied to several microcanonical unimolecular dissociations, e.g. Klippenstein *et al.* (1988) and Klippenstein & Marcus (1989, 1990) and other references cited later. Both the rate constants for dissociation and, with an added dynamical assumption (Marcus 1988), the rovibrational quantum state distributions of the reaction products have been so treated. The canonical rates of bimolecular association processes have similarly been studied.

In the present paper these applications to a number of systems are summarized, and compared with the experimental data and with the phase space theory (PST) of Pechukas & Light (1965) and Pechukas *et al.* (1966). PST, with its simplified ('loose') transition state, provides a very useful benchmark theory for comparison with more detailed theories and with the experimental data. The relation to other detailed theories such as that of Quack & Troe (1974, 1977) is discussed elsewhere (see, for example, Wardlaw & Marcus 1987). A two-transition-state formulation is also described and applied, in which the second transition state region consists of the orbital angular-momentum-dependent loose transition state of PST.

2. Transition state theory and variational RRKM

I first noted some time ago, in passing, a variational form of RRKM theory for reaction rates (Marcus 1966*a*). However, a computational way of implementing it for

Phil. Trans. R. Soc. Lond. A (1990) **332**, 283–296 *Printed in Great Britain*

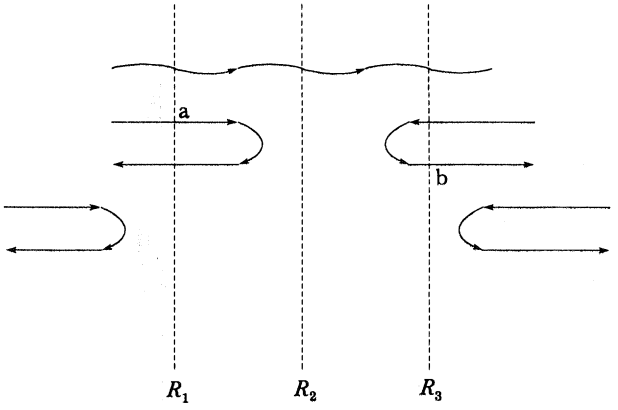

Figure 1. Example of crossing or recrossing of a hypersurface (e.g. at R_1, at R_2 and at R_3). Of the three hypersurfaces the one at R_2 has the least recrossing (none indicated), while those at R_1 and at R_3 show examples of a recrossing. For example, the points at a and at b count as forward motion in summing over phase space at R_1 and at R_2 respectively, but are wasted: they do not contribute successfully to the forward and reverse rates.

unimolecular dissociations was described only recently by Wardlaw & Marcus (1984, 1985, 1986, 1987) and Klippenstein & Marcus (1988*a*, *b*, 1990). The treatment is, in part, quantum mechanical, but it is useful to recall first a basis for a variational classical mechanical transition state theory. The latter is based on an early important, if for some time neglected, paper by Wigner (1938). Wigner pointed out that if a $(2N-1)$-dimensional surface in a $2N$-dimensional phase space could be found, separating the reactants region from the products region of phase space, such that no classical mechanical trajectories recrossed it, and if there was an equilibrium distribution in phase space for the reactants, transition state theory (TST) would be valid, within a classical mechanical framework: in a classical mechanical form of transition state theory it is tacitly assumed that all parts of the $(2N-1)$-dimensional dividing surface (a 'hypersurface'), which constitutes the transition state, contribute to the rate constant. If, instead, some of this $(2N-1)$-dimensional phase space is 'wasted', as reflected in some recrossing of it by trajectories, rather than their leading directly from reactants to products, the observed rate should be less than that predicted by TST. In this way Wigner established a theoretical basis for TST, which was, within its classical limitations, more fundamental than the more customary derivations present in texts.

It follows from such an argument that the best choice for the $(2N-1)$-dimensional dividing surface is the one with the fewest recrossings (cf. figure 1), i.e. the one with the minimum flux across it. A variational TST was proposed by Wigner (1937), Horiuti (1938) and Keck (1960, 1967). Finding such a dividing surface among the infinite number of possibilities, however, does present a formidable problem. In practice, some approximate choice is usually made for the 'reaction coordinate' R, and the latter then defines a family of parallel $(2N-1)$-dimensional dividing surfaces, the best one of which is determined variationally. Recent descriptions of a variational transition state theory have been given by Quack & Troe (1974, 1977), Hase (1972, 1983) and Garrett & Truhlar (1979), among others.

In the case of unimolecular dissociations Wigner's classical description of the motion is typically not adequate, since the vibrations in the transition state

are usually highly quantized, although the remaining degrees of freedom of the transition state can often be treated classically. Such a combined quantal-classical approach was used in our recent applications of variational RRKM theory to unimolecular dissociations (§3). The reaction coordinate is taken to be some separation distance, e.g. the centre-to-centre distance R of the separating fragments, or, as in Klippenstein (1990), a bond length, and the reactive flux across it is calculated, and then the R is found where that flux is a minimum. When the R-motion is treated classically the flux across any given R for any given total energy E and total angular momentum J, is proportional to the number of rovibrational quantum states $N_{EJ}(R)$ with energy equal to or less than E (Marcus 1966*b*). Minimization of $N_{EJ}(R)$ then yields the value of R, $R^{\ddagger}$, in the transition state.

3. Conserved and transitional modes in the transition state

In recent calculations of $N_{EJ}(R)$ the degrees of freedom of the dissociating molecule were classified by Wardlaw & Marcus (1984) as being of two types, the 'conserved' and the 'transitional' modes. The former are, typically, vibrations of the parent molecule which remain as vibrations in the separated fragments. The transitional modes are the remaining degrees of freedom, and include motions which were originally rocking vibrations of the two incipient fragments in the parent molecule (they become rotations of separated fragments) and include, also, the overall rotations. There are frequently eight transitional modes in the case of two polyatomic fragments, and they are typically highly coupled to each other and are constrained by the requirement of conservation of total angular momentum quantum number J.

The number of states $N_{EJ}(R)$ is then given by a convolution,

$$N_{EJ}(R) = \int_0^E N_v(E-\epsilon)\,\rho_J(\epsilon)\,\mathrm{d}\epsilon, \tag{3.1}$$

where $N_v(E-\epsilon)$ is the number of states of the conserved modes with an energy less than or equal to $E-\epsilon$, and is calculated by a direct count, and $\rho_J(\epsilon)$ is the density of states of the transitional modes and is treated classically by obtaining the amount of phase space available for the given ϵ and J. In practice, the right-hand side of (3.1) is evaluated by a Monte Carlo method.

Originally, the expressions for $\rho_J(\epsilon)$ were obtained by Wardlaw & Marcus (1984, 1986) in terms of action-angle variables, but later it was found possible by Klippenstein & Marcus (1988*a*, *b*) to express $\rho_J(\epsilon)$ in terms of conventional coordinates, while still satisfying the conditions of constant J (and constant component M of J) and having in (3.1) no extra integration variables than before.

Transition states range from 'tight' to 'loose' in nature. In the 'loose' transition state the separating fragments rotate freely, while in the 'tight' transition state they behave instead as they do in the parent molecule, namely undergo rocking vibrations. For the above classical treatment of $\rho_J(\epsilon)$ to be valid, the frequencies of 'transitional modes' should be small, which will occur when the transition state is closer to 'loose' than to 'tight'. This situation has been the case in the systems we have studied thus far. (For example, a calculation of quantum corrections for the transitional modes for the $C_2H_6 \rightarrow 2CH_3$ reaction using a path integral method by Klippenstein & Marcus (1987) showed the corrections to be small for that reaction.)

In RRKM theory the rate constant k_{EJ} for a dissociation at the given energy E and J is given by an expression (see, for example, Marcus 1952, 1965, 1970; Robinson & Holbrook 1972; Forst 1973)

$$k_{EJ} = N_{EJ}(R^{\ddagger})/h\rho_{EJ}, \tag{3.2}$$

where ρ_{EJ} is the density of states of the parent molecule at the given E and J; $R^{\ddagger}$, the now variationally-determined position of the transition state, depends on E and J and so is referred to as $R^{\ddagger}_{EJ}$ below. The observed unimolecular rate constant is obtained by summing (3.2) over any existing distribution of J and E.

We first compare, in the summary below, the results with those of PST. In PST the transition state is 'loose', i.e., the separated fragments rotate freely in the transition state, and so their orbital angular momentum quantum number l is a constant of the motion near the PST $R^{\ddagger}$ region. The $R^{\ddagger}$ in PST depends on l, and not explicitly on E or J, and will accordingly be denoted by $R^{\ddagger}_{l}$ instead of $R^{\ddagger}_{EJ}$. For any given J there is in PST a distribution of $R^{\ddagger}_{l}$s, since there is a distribution of ls. $R^{\ddagger}_{l}$ is typically rather large, occurring where the centrifugal force for the given l balances the long range (assumed radial) attractive force. Typically, the PST values of the reaction rate are larger than the variational RRKM values, because of the omission of PST of any steric restrictions in the transition state.

4. Rotational–vibrational quantum state distribution of separated fragments

Calculations have also been made of the rovibrational quantum state distribution of the reaction products of unimolecular dissociations. In PST it is assumed that for any given E and J all degrees of freedom are equilibrated by the time the system reaches the transition state at each $R = R^{\ddagger}_{l}$. Because of the assumed occurrence of freely rotating fragments in the transition state of PST, it follows that in PST the rovibrational quantum state distribution of the separated fragments is the same as that in the PST transition state. However, for RRKM theory some dynamical assumption or assumptions are needed, over and above its statistical assumptions used to calculate the rate constant k_{EJ}, to calculate a rovibrational quantum state distribution for the products. We consider here only reactions for which the potential energy V in the exit channel of the dissociating species rises monotonically to its value at $R = \infty$, rather than having some local maximum. In the latter case there would be still further dynamical forces influencing the quantum state distribution of the reaction products.

To calculate the products quantum state distributions using RRKM theory, dynamical assumptions were introduced (Marcus 1988) about the behaviour of the conserved vibrations and of the transitional modes after the system leaves the transition state. Because of their relatively high frequencies the conserved vibrations were assumed to behave adiabatically for Rs in the vicinity of and exceeding $R^{\ddagger}$. That is, their quantum numbers were assumed to be constants of the motion in this region. In this adiabatic treatment the $R^{\ddagger}$ can differ for each state i of the conserved modes and is denoted below by $R^{\ddagger}_{EJ,i}$. It occurs at the minimum of the reactive flux in state i, the reactive flux at R being proportional to $N_{EJ,i}(R)$, the total number of states, for the given state i, with a given J and with a total energy equal to or less than E. In spite of this assumed adiabaticity, there may be some subsequent recrossing of the

hypersurface $R = R^{\ddagger}_{EJ,i}$, as seen later when a two-transition state behaviour is treated with equations (4.3) and (4.4). I first describe, however, the one-transition state case, and later extend it to (4.3) and (4.4).

The dynamical assumption made for the transitional modes was quite different from the adiabatic one for conserved modes. Namely, in the region between $R^{\ddagger}_{EJ,i}$ and the PST $R^{\ddagger}$s a continuous equilibration rather than adiabaticity was assumed for the transitional modes (Marcus 1988). The energy level spacings of the transitional modes, e.g. of the hindered rotations, are on the average much smaller than those of the conserved vibrations: although the spacing of successive rotational states is $E_j - E_{j-1} = j\hbar^2/I$ for a freely rotating diatomic fragment, and so increases with j, the degeneracy of those states is $2j+1\,(\approx 2j)$. Thus, for hindered rotations in the transition state, where the m-degeneracy can be removed, the mean energy spacing of states is approximately $j\hbar^2/I(2j) = \hbar^2/2I$, which is typically small. This small spacing implies, semiclassically, small mechanical frequencies of the associated motion for the transitional modes, and so those modes are less apt to behave adiabatically. Consistent with this aspect it is assumed that any redistribution among the states of the transitional modes can occur readily in the region between $R^{\ddagger}_{EJ,i}$ and the PST $R^{\ddagger}$s, and, therefore that, as in PST, they remain equilibrated in the PST $R^{\ddagger}$ region. This 'non-adiabatic' assumption for the transitional modes contrasts with the adiabatic role assumed for all modes by Quack & Troe (1974, 1977) in their statistical adiabatic channel model.

One difference in the products rotational quantum state distribution in the present model from that in PST, seen from the above two dynamical assumptions, is that the rotational state quantum distribution of the fragments is now given by a conditional probability distribution. Given an RRKM-calculated distribution of vibrational states at $R^{\ddagger}_{EJ,i}$, the subsequent rotational state distribution for each vibrational state is the equilibrated rotational distribution at the relevant PST $R^{\ddagger}$s for the given state i of the conserved modes, as in (4.3) and (4.4) below. As part of this conditional probability, the distribution of rotational states at $R = \infty$ depends on whether some of the rotational channels that were open at $R^{\ddagger}_{EJ,i}$ are closed at the PST $R^{\ddagger}$s for the given E, J and i. The existence of such states is revealed by a comparison of the PST value of $N_{EJ,i}, N^{\mathrm{PST}}_{EJ,i}$, with the value at $R^{\ddagger}_{EJ,i}, N^{\ddagger}_{EJ,i}$. When the former is smaller than the latter, the total flux at the PSTs $R^{\ddagger}$s is also smaller, so that there has been some reflection before those PST $R^{\ddagger}$s were reached, i.e. some recrossing of the $R^{\ddagger}_{EJ,i}$ transition state occurred. One source of such recrossings is the existence of closed rotational channels at the PST $R^{\ddagger}$s, channels that were open at $R^{\ddagger}_{EJ,i}$. The formulation in Klippenstein & Marcus (1988*b*, 1990) allows for such recrossings.

Accordingly, in the vicinity of the threshold energy for excitation of a conserved mode i the following behaviour will ensue when $N^{\ddagger}_{EJ,i} > N^{\mathrm{PST}}_{EJ,i}$. At threshold for state i, the flux for this state i will be essentially zero, since all rotational channels but the lowest are closed at zero excess energy. As the energy is increased each successive rotational channel becomes open and a step-like population against energy plot results. At high enough excitation energies (typically *ca.* 100 cm^{-1} above threshold for each state i of the conserved modes, in the case of our calculations for $CH_2CO \rightarrow CH_2 + CO$), $N^{\mathrm{PST}}_{EJ,i}$ is no longer smaller than $N_{EJ,i}(R^{\ddagger}_{EJ,i})$. For slightly higher excess energies (*ca.* 200 cm^{-1} and above for this reaction), there is typically little further subsequent reflection of the dissociating systems in the PST $R^{\ddagger}$ region and it suffices to use only the $R^{\ddagger}_{EJ,i}$ transition state.

Using the above arguments, the population of a particular state (i,t) of the

conserved modes in state i and transitional modes in state t is given by the following expressions. In PST the flux yielding a particular quantum state (i,t) of the separated products is proportional to the number of states $N^{\mathrm{PST}}_{EJ,it}$ with total energy equal to or less than E and with this specification (i,t) at the PST $R^{\ddagger}_{l}$s. It includes a sum over all accessible ls. The normalized population $p^{\mathrm{PST}}_{EJ,it}$, is then given by

$$p^{\mathrm{PST}}_{EJ,it} = N^{\mathrm{PST}}_{EJ,it}/\sum_{i,t} N^{\mathrm{PST}}_{EJ,it}. \tag{4.1}$$

When a single transition state is used in the variational RRKM-based treatment of the products' quantum state distribution, the probability $p_{EJ,it}$ is given, instead, by

$$p_{EJ,it} = (N^{\ddagger}_{EJ,i}/\sum_{i} N^{\ddagger}_{EJ,i})\,(N^{\mathrm{PST}}_{EJ,it}/\sum_{t} N^{\mathrm{PST}}_{EJ,it}) \quad (\text{TS at } R^{\ddagger}_{EJ,i}). \tag{4.2}$$

When $N^{\ddagger}_{EJ,i} > N^{\mathrm{PST}}_{EJ,i}$ for any state i, where $N^{\mathrm{PST}}_{EJ,i}$ denotes $\Sigma_t N^{\mathrm{PST}}_{EJ,it}$, then $N^{\ddagger}_{EJ,i}$ in (4.2) is replaced by $N^{\mathrm{PST}}_{EJ,i}$ in this single-TS model.

The first factor in parentheses in (4.2) is the probability of finding the transition state in quantum state i of a conserved mode. The second factor is the conditional PST probability that, given that the system is in this state i, the system is found in state t of the transitional modes in the PST region.

When there are two bottlenecks, namely at $R^{\ddagger}_{EJ,i}$ and at the PST $R^{\ddagger}_{l}$s, equation (4.2) is modified to account for the fact that, particularly just above threshold for state i, some of the t-states which pass $R^{\ddagger}_{EJ,i}$ will be reflected in the PST transition state region. Instead of (4.2) we have, as in the present Appendix A,

$$p_{EJ,it} = (N^{\mathrm{eff}}_{EJ,i}/\sum_{i} N^{\mathrm{eff}}_{EJ,i})\,(N^{\mathrm{PST}}_{EJ,it}/\sum_{t} N^{\mathrm{PST}}_{EJ,it}) \quad (\text{composite TS}), \tag{4.3}$$

where

$$\frac{1}{N^{\mathrm{eff}}_{EJ,i}} = \frac{1}{N^{\ddagger}_{EJ,i}} + \frac{1}{N^{\mathrm{PST}}_{EJ,i}} - \frac{1}{N^{\mathrm{max}}_{EJ,i}}. \tag{4.4}$$

In the plot of $N_{EJ,i}(R)$ against R, $N^{\mathrm{max}}_{EJ,i}$ is the local maximum between the minima in $N_{EJ,i}(R)$ at $R^{\ddagger}_{EJ,i}$ and at the PST $R^{\ddagger}$s. When $N^{\mathrm{PST}}_{EJ,i}$ and $N^{\ddagger}_{EJ,i}$ are greatly different, for all i, equations (4.3) and (4.4) reduce to (4.2) (or to its counterpart for the $N^{\ddagger}_{EJ,i} > N^{\mathrm{PST}}_{EJ,i}$ case).

The position of the transition state in this two-transition-state RRKM-based model for determining the products quantum state distribution varies from being in the PST region, when the energy is just above the threshold for the vibrational excitation of state i, to being, at somewhat higher excess energies, in an inner region at $R^{\ddagger}_{EJ,i}$. In general the transition state is a composite one, as in (4.3) and (4.4). This shift of the transition state plays an important role in our interpretation later of photofragmentation spectra (§5c).

Corresponding to (4.1)–(4.3) the distribution of the i-states of the products is obtained from them by summing over t in each of those expressions:

$$p^{\mathrm{PST}}_{EJ,i} = \sum_{t} N^{\mathrm{PST}}_{EJ,it}/\sum_{i,t} N^{\mathrm{PST}}_{EJ,it} = N^{\mathrm{PST}}_{EJ,i}/\sum_{i} N^{\mathrm{PST}}_{EJ,i}, \tag{4.5}$$

$$p_{EJ,i} = N^{\ddagger}_{EJ,i}/\sum_{i} N^{\ddagger}_{EJ,i}, \tag{4.6}$$

$$p_{EJ,i} = N^{\mathrm{eff}}_{EJ,i}/\sum_{i} N^{\mathrm{eff}}_{EJ,i}. \tag{4.7}$$

Given some knowledge or estimate of the potential energy surface in the transition state region, a calculation of $N_{EJ}(R)$ using (3.1) and the various $N^{\ddagger}_{EJ}$s in the above equations becomes practical and relatively straightforward, and has been done for a number of reactions. Some knowledge is needed, particularly of the potential energy surface for the transitional modes in the vicinity of the nearly loose transition state. In the calculations an effort was made to avoid adjustable parameters: non-bonded interactions were estimated according to some available prescription. The bonded interaction potential for the dissociating bond was obtained by subtracting from an 'experimental' bond potential the contribution of the non-bonded interactions in the most stable molecular configuration at each R. When available such estimates can later be compared with the results of more *ab initio* calculations for each system, as in the comparison of Darvesh *et al.* (1989) with Wardlaw & Marcus (1985).

5. Results

(*a*) *Bimolecular association rates*

One of the systems that has been treated with variational RRKM is the recombination of methyl radicals. Here, the high pressure rate constant $k_{\mathrm{bi}}(T)$ can be calculated using the above formalism for k_{EJ} for the dissociation. Upon thermally averaging over E and J at the given T the unimolecular rate constant $k_{\mathrm{uni}}(T)$ is obtained, and then with use of similar information the equilibrium constant, $k_{\mathrm{bi}}(T)$ can be calculated. The value obtained for $k_{\mathrm{bi}}(T)$ when T was varied from about 300 K to about 1200 K decreased by about a factor of roughly two, as in Wardlaw & Marcus (1987) and Darvesh *et al.* (1989), and appears to be consistent with available high-pressure limit data. (References to the experimental data are cited in Wardlaw & Marcus (1986), Wagner & Wardlaw (1988) and in Darvesh *et al.* (1989).) Phase space theory, on the other hand, leads to a $k_{\mathrm{bi}}(T)$ which varies as $T^{\frac{1}{6}}$ and so increases rather than decreases with temperature. In PST the average position of the transition states is shifted to slightly smaller $R^{\ddagger}_{l}$s with increasing $T(\langle R^{\ddagger}\rangle \propto T^{-\frac{1}{6}})$, as seen in Appendix B, but this effect is more than compensated by the effect of temperature causing an increased mean velocity for crossing the centrifugal plus attractive force barrier (Appendix B). In variational RRKM theory the mean position of the transition state is also shifted to smaller $R^{\ddagger}$s as T is increased, but even more so: the larger spacing of the hindered rotational states at smaller R typically lowers the $N_{EJ}(R)$ curve more than at larger R and enhances the shift of $R^{\ddagger}$ to smaller values at high Ts. This effect, and the enhanced steric restrictions in the TS that results, usually causes $k_{\mathrm{bi}}(T)$ for recombination to decrease with increasing temperature.

Another example of a bimolecular recombination process is the reaction between NC and O_2, studied by Sims & Smith (1988), which is believed to proceed via some intermediate NCOO, an analogue of NCNO. Here, $k_{\mathrm{bi}}(T)$ showed a significant decrease (roughly a factor of almost 3) when the temperature T was increased from 100–765 K. Calculations of $k_{\mathrm{bi}}(T)$ based on long range attractive potential (dipole–quadrupole) was shown by Clary (1984) to give rise only to a relatively small decrease of $k_{\mathrm{bi}}(T)$ with increasing temperature. The effects of non-bonded interactions may well, as in the $2CH_3 \rightarrow C_2H_6$ recombination, lead to a larger temperature coefficient, judging from some unpublished results in our group for the NC + NO recombination. It is planned to explore this matter further.

Variational RRKM calculations for $CH_3 + H$ recombination have been made by Aubanel & Wardlaw (1989). The value of $R^{\ddagger}$ again shifted to smaller values with

increasing temperature, the decrease being somewhat less than that for the CH_3+CH_3 recombination. The calculated rate showed, however, an increase with increasing temperature, as does that of PST, instead of the decrease found for $2CH_3$, and perhaps reflecting, in part, the fewer and less restricted hindered rotors in the CH_3+H transition state. The experimental data for $CH_3+H \rightarrow CH_4$ are not yet sufficiently established to make an adequate comparison with those calculations. Detailed studies of the CH_3+H recombination, using various potential energy surfaces, have been made by Hu & Hase (1989).

(*b*) *Unimolecular dissociation rates*

Experimental measurements of microcanonical rates of the $NCNO \rightarrow NC+NO$ dissociation have been described by Khundkar *et al.* (1987), and for the $CH_2CO \rightarrow CH_2+CO$ dissociation by Potter *et al.* (1989). Theoretical studies with variational RRKM theory have been given for the microcanonical rates of the NCNO dissociation by Klippenstein *et al.* (1988) and of the CH_2CO dissociation by Klippenstein & Marcus (1989). In the NCNO system, photoexcitation to the S_1 state is followed by internal conversion to the S_0 state, with some contribution to the reaction from triplet states. In the case of PST, when all final states were included without regard to the nature of the potential energy function (a local maximum in the triplet state) in the intervening region, the calculation of the microcanonical rate constants k_{EJ} exceeded the experimental values by a factor of ten or so at the higher energies in the excess energy interval studied, 0–700 cm^{-1}. Inclusion by Klippenstein *et al.* (1988) of the locally high barriers for the exit channel for all but the S_0 state suggested that at these low excess energies only the S_0 states need be considered (provided there is negligible S–T intersystem crossing at larger Rs). When this feature was included in the PST calculation, the PST results were quite close to those for variational RRKM. Thus, at these energies the RRKM transition state is rather loose.

The experimental results for the microcanonical $NCNO \rightarrow NC+NO$ dissociation by Khundkar *et al.* (1987) are shown in figure 2, where they are compared with variational RRKM theory. The results are seen to be quite close. Experimental results for k_{EJ} at higher energies would be useful. Since at *ca.* 700 cm^{-1} excess energy the lifetime is still *ca.* 10 ps, shorter lifetimes could presumably be studied.

Photoexcitation of CH_2CO, yields the singlet S_1 state, which is followed by internal conversion to S_0, as well as by intersystem crossing to the triplet T_1. The T_1 state has a local maximum in the potential energy curve in the exit channel. In the excess energy range investigated (*ca.* 100–6000 cm^{-1} above the singlet dissociation energy threshold) most of the reaction appeared to proceed via the singlet state, and use of the latter sufficed for comparison with the experimental results on the dissociation rates. The experimental results of Potter *et al.* (1989) are given in figure 3.

Comparing PST and RRKM calculations for the singlet surface for CH_2CO there was a considerable difference in the two k_{EJ}s (Klippenstein & Marcus 1989), the PST value being some eight times higher at the higher end of this energy range, as in figure 3. Even at a 500 cm^{-1} excess energy there is seen to be already a factor of about five difference between PST and RRKM; at the low end of the range at 100 cm^{-1} the ratio is 1.3. In part, the difference between the PST and RRKM k_{EJ} results for CH_2CO, compared with their being close to each other for NCNO, appears to be due to the shorter range interaction of CH_2 and CO, resulting in stronger hinderance of the rotations at $R^{\ddagger}_{EJ}$. The rotational motion of the CH_2 about its mass centre also appears

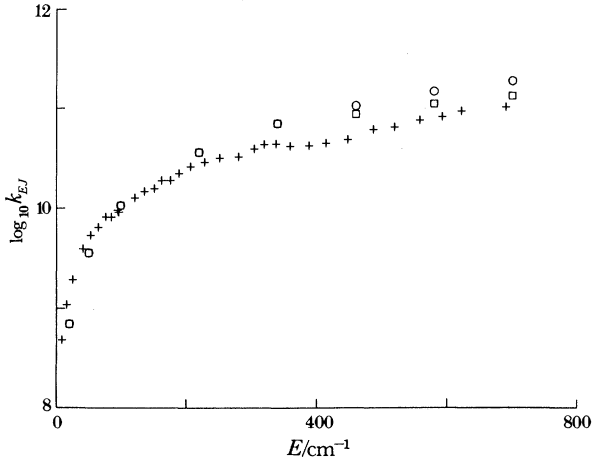

Figure 2. Plot of $\log_{10} k_{EJ}$ for NCNO dissociation against excess energy E. The pluses denote the experimental results of Khundkar *et al.* (1987) and the circles and squares refer to the use of two different potential energy functions in variational RRKM theory (figure 4 of Klippenstein *et al.* 1988).

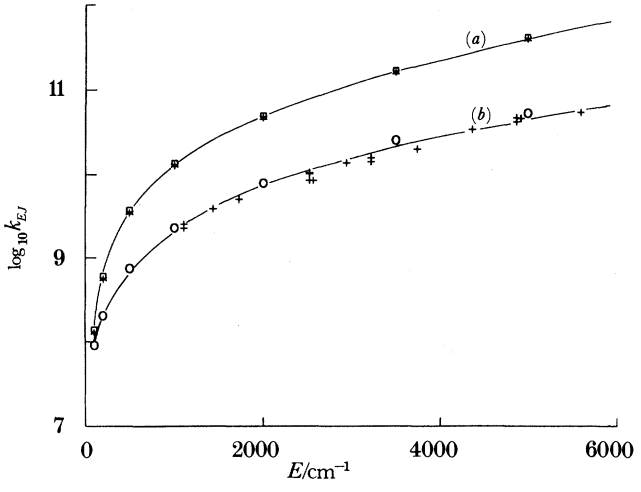

Figure 3. Plot of $\log_{10} k_{EJ}$ for CH_2CO dissociation against excess energy E. The pluses denote the experimental results of Potter *et al.* (1989), the open circles the variational RRKM results and the upper curve describes the classical (crosses) and quantal (boxes) PST results (figure 2 of Klippenstein & Marcus 1989). (*a*) PST, (*b*) experimental RRKM.

to involve a larger asymmetry in its interaction with CO than is apparently the case in the NC + NO case, and so causes a larger difference between PST and RRKM results in $CH_2CO \rightarrow CH_2 + CO$.

The experimental, PST and RRKM results for CH_2CO are given in figure 3. The variational RRKM treatment yields substantially better agreement with the experimental data of Potter *et al.* (1989), reflecting the presence of steric hindrance in the transition state.

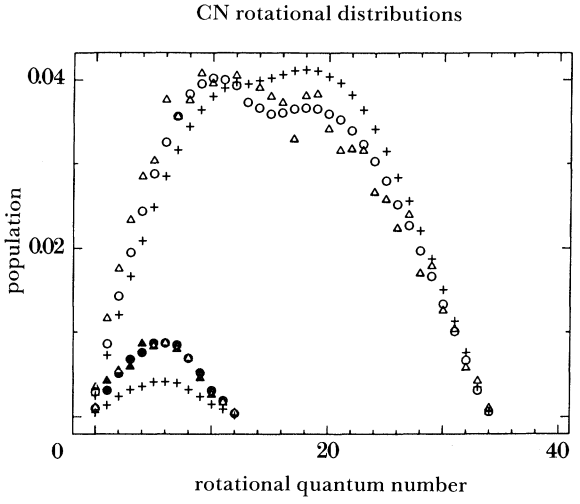

Figure 4. Plot of relative CN rotational state population for both the $v = 0$ and $v = 1$ CN vibrational states resulting from the dissociation of NCNO at an excess energy of 2348 cm^{-1}. For $v = 0$ (the three upper set of points) the triangles denote experimental results of Wittig *et al.* (1985), the circles denote RRKM-based results and the pluses those of PST. For $v = 1$, the triangles denote experimental results (using data from H. Reisler) the circles the RRKM-based results and the pluses the PST results (fig. 15 of Klippenstein *et al.* 1988).

(c) *Distribution of quantum states of the separated fragments*

At subvibrational excitation energies of the products of a dissociation, the results for variational RRKM theory (with the dynamical exit channel assumptions discussed earlier) for the products' quantum state distribution are the same as those of PST, as seen from a comparison of (4.1) and (4.2). The first factor in the right-hand side of (4.2) is unity at those energies. When instead the excess energy is sufficient to excite the products vibrationally there can be additional vibrational excitation, over and above that expected from PST (Klippenstein *et al.* 1988; Klippenstein & Marcus 1989, 1990).

Experimental results for the NCNO dissociation were reported by Qian *et al.* (1985) and Wittig *et al.* (1985) for the CN and NO quantum state distributions. Results were obtained both at low excess energies (95–940 cm^{-1} above threshold), below the vibrational excitation threshold of the products, and for higher excess energies (2348–4269 cm^{-1}) where some of the products were vibrationally excited to a $v_{CN} = 1$ or a $v_{NO} = 1$ state. The data for NCNO at subvibrational products excitation energy showed good agreement with both theories; at those excitations the two theories for the product state distribution agree with each other. At excitations permitting the vibrational excitation of the products, the RRKM + dynamical assumption model shows better agreement with the data, in comparison with PST, as in figure 4, but at the higher energies the two sets of results approached each other (Klippenstein *et al.* 1988).

Results on products quantum state distribution for CH_2CO dissociation have been obtained by Chen *et al.* (1988) and by Green *et al.* (1988, 1990). For $CH_2CO \rightarrow CH_2 + CO$ the photofragmentation excitation spectra (PHOFEX) have been studied. Here, the appearance threshold of individual rotational states of the products have been determined, superimposed on a vibrational excitation, as in figure 5. The step-

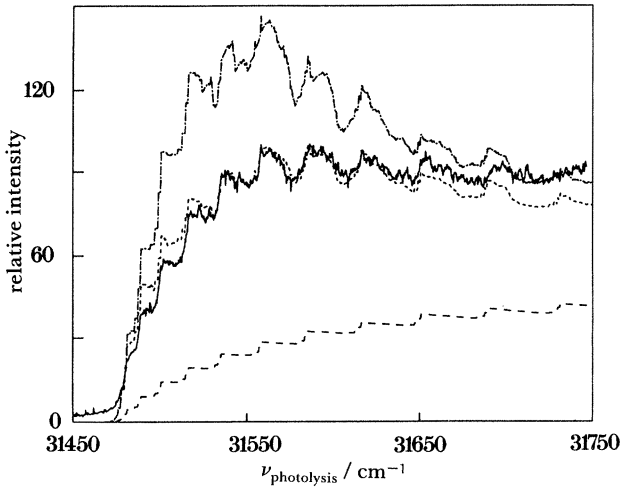

Figure 5. Photofragment excitation spectrum for the $v_{HCH} = 1$, $J_{K_aK_c} = 1_{01}$ vibrational–rotational state of methylene formed from CH_2CO. The experimental results (Green *et al.* 1990) are given by the solid line, the PST results based on (4.1) by the long-dashed line (the lowest line), the absolute minimum RRKM-based results (cf. equation (4.2)) by the dot-dashed lines (highest line), and the RRKM-based treatment based on (4.3) by the short dashed line (the line which most closely follows the experimental trend). The excess energy ranges from approximately 1335 cm^{-1} to 1635 cm^{-1}.

like nature of the PHOFEX spectra reflects the quantized behaviour of the individual rotational states of the products. Typical calculated results are given in Klippenstein & Marcus (1990), and the three expressions (4.1), (4.2) and (4.3), (4.4) are illustrated in figure 5, scaled so that (4.3) and (4.4) agrees with the experimental data near the maximum in the latter. (Additional examples are given in that reference.) Poorer results for the shape of the plots were obtained when the scaling was based, instead, on (4.1) or (4.2). Equations (4.3) and (4.4) also gave better agreement than the PST (4.1) for the yield of vibrationally-excited products.

Interestingly enough, although the two-TS model plays, in this view, an important role for a PHOFEX spectrum near any i-state threshold, its role in the calculation of k_{EJ} was minor, as in Klippenstein *et al.* (1988) and Klippenstein & Marcus (1989), except at the threshold for k_{EJ} itself. Typically, the contribution to k_{EJ} from i states at their thresholds at any E is appreciably less than that of the non-threshold i states, in the systems studied.

6. Summary

In summary, studies for various reactions have shown interesting comparisons of the experimental data and theory for reaction rates and for the distributions of quantum states of the products. Using variational RRKM theory and its extension to include some dynamics in the post transition state region, to permit a treatment of the products quantum state distribution, it has been possible to obtain a unified basis for treating both types of data. It would be of particular interest to extend the experimental studies to other systems, to explore the generality, if any, of the trends found thus far in the present series of studies discussed above.

It is a pleasure to acknowledge the support of this research by the National Science Foundation, and helpful discussions with S. J. Klippenstein.

Appendix A. Derivation of equations (4.3) and (4.4)

Hirschfelder & Wigner (1939) showed that if there are two transition states, i.e. two regions, not just one, where a transmission or reflection of the reacting flux can occur and that if κ_1 and κ_2 denoted the transmission probabilities, the net transmission probability κ for reaction is given by

$$\kappa = \frac{\kappa_1 \kappa_2}{1-(1-\kappa_1)(1-\kappa_2)}. \tag{A 1}$$

Miller (1976) pointed out that each κ_i, a ratio of fluxes, could be written as a ratio of numbers of states:

$$\kappa_1 = N_1^{\ddagger}/N^{\max}, \quad \kappa_2 = N_2^{\ddagger}/N^{\max}, \tag{A 2}$$

where $N_1^{\ddagger}$ is the number of quantum states at transition state 1 with energy equal to or less than E, $N_2^{\ddagger}$ is the corresponding quantity at transition state 2, and $N^{\max}$ is the local maximum in N between $R_1^{\ddagger}$ and $R_2^{\ddagger}$.

Equations (4.3) and (4.4) are essentially an extension of (A 1) and (A 2). In the present case transition state 2 is, instead, a set of PST transition states, each transition state with its own value of l. That is, there will be reflection at various alternative, mutually exclusive, $R_l^{\ddagger}$s in the transition state region 2. $N_1^{\ddagger}$, the sum of the numbers of states over all l contributions, is denoted here by N^{PST}. Upon further specializing the reacting systems considered to those of a particular E, J, and i, as in Klippenstein & Marcus (1989), the present equations (4.3) and (4.4) are obtained.

Multiple transition states for the unimolecular dissociations of ions have been discussed by Chesnavich (1986) and by Jarrold *et al.* (1984) and are closely related to the subject matter of this Appendix.

Appendix B. Phase space theory $\langle R_l^{\ddagger} \rangle$

In phase space theory a transition state, $R = R_l^{\ddagger}$, is considered for each l. At the PST transition state the attractive force, $-\partial V(R)/\partial R$ and the centrifugal force $\partial/\partial R(L^2/2\mu R^2)$ just balance. (L, the total angular momentum is $(l(l+1)\hbar^2)^{\frac{1}{2}}$ which we can approximate below as $l\hbar$ for brevity.) Thus, at any E and J there are many $R_l^{\ddagger}$s because there is a distribution of ls. We can define some average $R_l^{\ddagger}$ at a given E and J, or since, in the relevant discussion in the text we were interested in knowing how an average $R_l^{\ddagger}$ in PST varies with temperature, we examine that quantity instead.

In this form, the PST model for the dependence of a bimolecular association reaction rate on temperature, rather than on E and J, reduces to the theory of Gorin (1938), in which the separated fragments rotate freely in the transition state.

For the bimolecular reaction rate constant we then have in the standard way

$$k_{\mathrm{bi}}^{\mathrm{PST}}(T) = \left(\int_0^{\infty} \frac{\exp\left[-(V_{\mathrm{eff}})/k_B T\right](2l+1)\,\mathrm{d}l}{2\pi\mu kT/h^2} \right) \left(\int_0^{\infty} \frac{\exp\left[-p^2/2\mu k_B T\right](p/\mu h)\,\mathrm{d}p}{(2\pi\mu kT)^{\frac{1}{2}}/h} \right), \tag{B 1}$$

where V_{eff} denotes $V(R)+L^2/2\mu R^2$, evaluated at the maximum of $V_{\mathrm{eff}}(R)$, and depends only on l and on the properties of $V(R)$. The rovibrational partition functions of the transition state in the numerator and that of the reactants in the denominator cancelled in (B 1), since the fragments rotate freely in the PST transition state.

The second factor on the right-hand side of (B 1) equals $(kT/2\pi\mu)^{\frac{1}{2}}$ and represents the velocity-weighted factor for crossing the transition state region. In the first factor on the right-hand side of (B 1), for a $V(R)$ which is AR^{-6}, the $\partial/\partial R(V_{\text{eff}})$ is zero at $R = R_l^{\ddagger}$, where $R_l^{\ddagger}$ equals $(6A\mu/L^2)^{\frac{1}{4}}$. Equation (B 1) then yields

$$k_{\text{bi}}^{\text{PST}}(T) = \left(\frac{2\pi}{\mu k_B T}\int_0^{\infty} \exp\left[-(L^3/Ck_B T)\right] \mathrm{d}L^2\right)\left(\frac{k_B T}{2\pi\mu}\right)^{\frac{1}{2}} \tag{B 2}$$

where the constant C denotes $3(6A\mu^3)^{\frac{1}{2}}$.

Several consequences follow from this expression: it is seen that L^3 scales with T as $k_B T$ and so the first parentheses' factor in (B 2) varies as $(k_B T)^{\frac{2}{3}}/k_B T$, i.e. as $(k_B T)^{-\frac{1}{3}}$. Thus, the $(k_B T)^{\frac{1}{2}}$ from the second parentheses' factor more than compensates for this inverse temperature dependence, and yields the well-known $T^{\frac{1}{6}}$ dependence for $k_{\text{bi}}^{\text{PST}}(T)$. Further since L^3 scales as $k_B T$ and $R_l^{\ddagger}$ was seen above to vary as $L^{-\frac{1}{2}}$, $R_l^{\ddagger}$ scales as $T^{-\frac{1}{6}}$. More precisely, the average $R_l^{\ddagger}$, given by (B 3), varies as $T^{-\frac{1}{6}}$, and so shifts to smaller values with increasing T, as noted in the text and in Rai & Truhlar (1983):

$$\langle R_l^{\ddagger}\rangle = \int_0^{\infty} (6A\mu/L^2)^{\frac{1}{4}} \exp\left[-\frac{L^3}{Ck_B T}\right] \mathrm{d}L^2 \Big/ \int_0^{\infty} \exp\left[-\frac{L^3}{Ck_B T}\right] \mathrm{d}L^2. \tag{B 3}$$

References

Aubanel, E. E. & Wardlaw, D. M. 1989 *J. phys. Chem.* **93**, 3117–3124.

Chen, I.-C., Green, W. H., Jr & Moore, C. B. 1988 *J. chem. Phys.* **89**, 314–328.

Chesnavich, W. J. 1986 *J. chem. Phys.* **84**, 2615–2619.

Clary, D. C. 1984 *Molec. Phys.* **53**, 3–21.

Darvesh, K. V., Boyd, A. J. & Pacey, P. D. 1989 *J. chem. Phys.* **93**, 4772–4779.

Forst, W. 1973 *Theory of unimolecular reactions*. New York: Academic Press.

Garrett, W. H. & Truhlar, D. G. 1979 *J. chem. Phys.* **70**, 1593–1598.

Gorin, E. 1938 *Acta Physiochim. U.R.S.S.* **9**, 681–696.

Green, W. H., Jr, Chen, I.-C. & Moore, C. B. 1988 *Ber. Bunsenges. Phys. Chem.* **92**, 389–396.

Green, W. H., Jr, Mahoney, A. J., Cheng, C.-K. & Moore, C. B. 1990 (In preparation.)

Hase, W. L. 1972 *J. chem. Phys.* **57**, 730–733.

Hase, W. L. 1983 *Acc. Chem. Res.* **16**, 258–264.

Hirschfelder, J. O. & Wigner, E. 1939 *J. chem. Phys.* **7**, 616–628.

Horiuti, J. 1938 *Bull. Chem. Soc. Japan* **13**, 210–216.

Hu, X. & Hase, W. L. *J. phys. Chem.* **93**, 6029–6038.

Jarrold, M. F., Wagner-Redeker, W., Illies, A. J., Kirchner, N. J. & Bowers, M. T. 1984 *Int. J. Mass Spectr. Ion Proc.* **58**, 63–95.

Keck, J. C. 1960 *J. chem. Phys.* **32**, 1035–1050.

Keck, J. C. 1967 *Adv. chem. Phys.* **13**, 85–121.

Khundkar, L. R., Knee, J. L. & Zewail, A. H. 1987 *J. chem. Phys.* **87**, 77–96.

Klippenstein, S. J. & Marcus, R. A. 1987 *J. chem. Phys.* **87**, 3410–3417.

Klippenstein, S. J. & Marcus, R. A. 1988*a* *J. phys. Chem.* **92**, 3105–3109.

Klippenstein, S. J. & Marcus, R. A. 1988*b* *J. phys. Chem.* **92**, 5412–5417.

Klippenstein, S. J., Khundkar, L. R., Zewail, A. H. & Marcus, R. A. 1988 *J. chem. Phys.* **89**, 4761–4770.

Klippenstein, S. J. & Marcus, R. A. 1989 *J. chem. Phys.* **91**, 2280–2292.

Klippenstein, S. J. & Marcus, R. A. 1990 *J. chem. Phys.* (In the press.)

Klippenstein, S. J. 1990 *Chem. Phys. Lett.* (In the press.)
Marcus, R. A. 1952 *J. chem. Phys.* **20**, 359–364.
Marcus, R. A. 1965 *J. chem. Phys.* **43**, 2658–2661.
Marcus, R. A. 1966*a* *J. chem. Phys.* **43**, 2630–2638.
Marcus, R. A. 1966*b* *J. chem. Phys.* **45**, 2138–2144.
Marcus, R. A. 1970 *J. chem. Phys.* **52**, 1018.
Marcus, R. A. 1988 *Chem. Phys. Lett.* **144**, 208–214.
Miller, W. H. 1976 *J. chem. Phys.* **65**, 2216–2223.
Pechukas, P. & Light, J. C. 1965 *J. chem. Phys.* **42**, 3281–3291.
Pechukas, P., Light, J. C. & Rankin, C. 1966 *J. chem. Phys.* **44**, 794–805.
Potter, E. D., Gruebele, M., Khundkar, L. R. & Zewail, A. H. 1989 *Chem. Phys. Lett.* **164**, 463–470.
Qian, C. X. W., Noble, M., Nadler, I., Reisler, H. & Wittig, C. 1985 *J. chem. Phys.* **83**, 5573–5580.
Quack, M. & Troe, J. 1974 *Ber. BunsenGes. Phys. Chem.* **78**, 240–252.
Quack, M. & Troe, J. 1977 *Ber. BunsenGes. Phys. Chem.* **81**, 329–337.
Rai, S. N. & Truhlar, D. G. 1983 *J. chem. Phys.* **79**, 6049–6058.
Robinson, P. J. & Holbrook, K. A. 1972 *Unimolecular reactions*. New York: Wiley-Interscience.
Sims, I. R. & Smith, I. W. M. 1988 *Chem. Phys. Lett.* **151**, 481–484.
Wagner, A. F. & Wardlaw, D. M. 1988 *J. phys. Chem.* **92**, 2462–2471.
Wardlaw, D. M. & Marcus, R. A. 1984 *Chem. Phys. Lett.* **110**, 230–234.
Wardlaw, D. M. & Marcus, R. A. 1985 *J. chem. Phys.* **83**, 3462–3480.
Wardlaw, D. M. & Marcus, R. A. 1986 *J. phys. Chem.* **90**, 5383–5393.
Wardlaw, D. M. & Marcus, R. A. 1987 *Adv. chem. Phys.* **70** (1), 231–263.
Wigner, E. 1937 *J. chem. Phys.* **5**, 720–725.
Wigner, E. 1938 *Trans. Faraday Soc.* **34**, 29–41.
Wittig, C., Nadler, I., Reisler, H., Noble, M., Catanzarite, J. & Radhakrishnan, G. 1985 *J. chem. Phys.* **83**, 5581–5588.

PHILOSOPHICAL TRANSACTIONS OF THE ROYAL SOCIETY A MATHEMATICAL, PHYSICAL & ENGINEERING SCIENCES